AJNR

CT Angiographic Source Images: Flow- or Volume-Weighted?

M. Sharma, A.J. Fox, S. Symons, A. Jairath and R.I. Aviv

AJNR Am J Neuroradiol 2011, 32 (2) 359-364
doi: https://doi.org/10.3174/ajnr.A2282
http://www.ajnr.org/content/32/2/359

ORIGINAL RESEARCH

CT Angiographic Source Images: Flow- or Volume-Weighted?

M. Sharma
A.J. Fox
S. Symons
A. Jairath
R.I. Aviv

BACKGROUND AND PURPOSE: CTA-SI have been previously reported to correlate with CBV. We hypothesized that CTA-SI performed by modern multisection CT scanners are CBF-, not CBV-weighted.

MATERIALS AND METHODS: Sixty-four consecutive patients with anterior circulation stroke symptoms were selected from a stroke data base between June 2007 and January 2009. Two independent blinded readers calculated defect volumes of CTA-SI and PCCT, CBF, and CBV images. Spearman correlation of lesion volumes was performed. Linear regression and residual analysis demonstrated factors associated with outliers for CTA or PCCT for CBF and CBV volumes.

RESULTS: We found a strong positive correlation between CTA with CBF ($r = 0.89$, $P < .0001$) and between PCCT and CBV ($r = 0.79$, $P < .0001$). CTA to CBV ($r = 0.5$, $P < .0001$) and PCCT to CBF ($r = 0.52$, $P < .0001$) correlations were weaker. Positive CTA outliers had lower ASPECTS ($P = .01$), larger baseline CTA (149 ± 46 cm^3 versus 83 ± 32 cm^3; $P = .002$, respectively), and final infarct (190 ± 100 cm^3 versus 80 ± 50 cm^3; $P = .09$, respectively) volumes than nonoutliers. No baseline features were significantly related to PCCT outliers. There was no difference in the vessel occlusion sites for positive or negative outliers for CTA or PCCT ($P = .55$ and $P = 1.00$, respectively).

CONCLUSIONS: Our results indicate that CTA-SI are CBF- rather than CBV-weighted.

ABBREVIATIONS: ACA = anterior cerebral artery; ASPECTS = Alberta Stroke Program Early CT Score; AUC = area under the curve; CBF = cerebral blood flow; CBV = cerebral blood volume; CTA = CT angiography; CTA-SI = CT angiographic source images; DWI = diffusion-weighted imaging; ICA = internal carotid artery; IQR = interquartile range; log = log-transformed; MCA = middle cerebral artery; MDCT = multidetector row CT; min = minutes; NCCT = noncontrast CT; NIHSS = National Institutes of Health Stroke Scale; PCCT = postcontrast CT; Q1–Q3 = interquartiles 1–3; rtPA = recombinant tissue plasminogen activator

CT is recommended as the technique of choice for initial stroke imaging work-up.[1,2] Semiquantitative methods such as the ASPECTS are reliable and convenient for visual assessment of baseline lesion volume on CT.[3,4] CTA-SI, reconstructed from the source data, are an important adjunct to acute stroke imaging assessment. Hypoattenuation of CTA-SI on earlier generation scanners has been correlated with DWI abnormality,[5] better predicting final infarct volume than NCCT alone. CTA-SI are suggested for the assessment of tissue infarct extent in the absence of DWI, with increased sensitivity in less experienced readers.[6-10] Baseline CTA source image abnormality was previously reported to closely match final infarct volume on follow-up imaging after successful recanalization.[11] This observation was confirmed by a later study using ASPECTS assessment on CTA-SI to predict final infarct size.[9,11]

Hypoattenuation on CTA-SI differs from early ischemic changes seen on NCCT and is thought to represent regions of reduced CBV,[9] rather than cytotoxic edema.[10] It is increasingly accepted that NCCT, CTA-SI, and CBV maps represent unsalvageable tissue despite reperfusion.[12] It has been a general observation in our stroke imaging practice that the observed hypoattenuation on CTA-SI is often larger than the CBV deficit on perfusion CT and more closely correlates with the CBF defect. A recent review indicated that despite theoretic modeling suggesting CTA-SI to be predominantly blood-volume weighted, the more rapid modern MDCT CTA protocols may be too quick to achieve arterial and tissue contrast steady-state and are more likely blood-flow-weighted.[13]

The aim of the present study was to correlate CTA-SI and PCCT hypoattenuation with perfusion CT–derived CBF and CBV abnormalities. We hypothesized that CTA-SI correlate more closely with CBF abnormalities, whereas PCCT would more closely correlate with CBV defects.

Materials and Methods

Study Design and Patient Cohort

All study procedures and medical chart reviews were approved by the research ethics board. All patients presenting with anterior circulation stroke symptoms within 3 hours, or their substitute decision-maker when appropriate, signed consent for prospective enrollment into a dedicated stroke data base at a regional stroke center. Consecutive patients completing a stroke imaging protocol between June 2007 and January 2009 were retrospectively selected for study analysis. A total of 64 patients were selected from 135 patients. Forty-seven patients were excluded due to poor CTA-SI/PCCT to average map

Received March 18, 2010; accepted after revision July 9.

From the Department of Medical Imaging, University of Toronto and Sunnybrook Health Sciences Centre, Toronto, Ontario, Canada.

Paper previously presented as a poster at: Annual Meeting of the American Society of Neuroradiology, May 15–20, 2010; Boston, Massachusetts.

Please address correspondence to Richard I. Aviv, MD, Sunnybrook Health Sciences Centre, 2075 Bayview Ave, Room AG 31, Toronto, ON, Canada M4N 3M5; e-mail: richard.aviv@sunnybrook.ca

Indicates article with supplemental on-line tables.

DOI 10.3174/ajnr.A2282

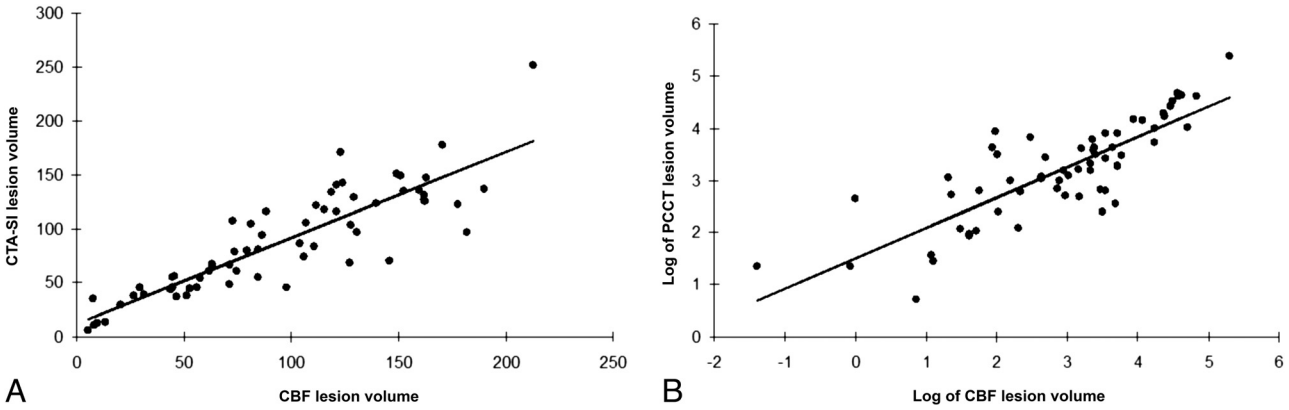

Fig 1. *A*, Fitted regression line and scatterplot of hypoattenuation volumes of CTA-SI and CBF defect volumes in cubic centimeters. *B*, logPCCT hypoattenuation volumes and logCBV defect volumes.

coregistration. A city-wide policy mandates that patients, initially diverted from their geographically closest hospital to our tertiary stroke center, be repatriated following acute care delivery. Twenty-one patients were sent back before obtaining recanalization data. Three studies were excluded due to patient motion. Baseline demographic data, including age, sex, ASPECTS, NIHSS score, time to scanning, rtPA dose, and site of vessel occlusion, were recorded and prospectively entered into a stroke data base. A single reader (M.S.) also noted the time difference between "smart" preparation completion and the midinfarct level. This parameter is recorded on the header of each image, and the difference was obtained by subtracting the 2 times and was recorded in seconds.

Scan Protocol

CT stroke protocol was performed on a 64-section CT scanner (Lightspeed VCT; GE Healthcare, Waukesha, Wisconsin) and included perfusion CT with 4-cm z-plane coverage and a CTA from the aortic arch to the vertex. Pre- and postcontrast CT head parameters were the following: 120 kV(peak), 340 mA, 8 × 5 mm collimation, 1 s/rotation, and a table speed of 15 mm/rotation. PCCT was performed immediately following CTA and perfusion CT, which was approximately 2 minutes following the initial contrast injection. CTA parameters were the following: 0.7 mL/kg of iodinated contrast agent up to a maximum of 90 mL (iohexol, Omnipaque, 300 mg iodine/mL; GE Healthcare, Piscataway, New Jersey); 5 mL/s injection rate; 5- to 10-second delay; 120 kVp; 270 mA; 1 s/rotation; 1.25-mm-thick sections; and table speed, 3.7 mm/rotation. Perfusion CT study parameters were 80 kVp, 190 mA, 8 × 5 mm collimation, and 1 s/rotation. Iodinated contrast agent at a dose of 0.5 mL/kg (maximum, 50 mL) was injected 3–5 seconds before the start of the first phase at a rate of 4 mL/s. A single operator (R.I.A., with 6 years' experience) used CT Perfusion 4 (GE Healthcare) to calculate parametric maps of CBF, CBV, and mean transit time. Arterial input and venous output functions were obtained from the ipsilateral anterior cerebral artery and from the superior sagittal sinus, respectively. Partial volume averaging of the arterial input curve was corrected by scaling the curve with the ratio of the AUC of the venous output curve to the AUC of the arterial input curve.[14] Maps were calculated by deconvolution of the arterial input curve and tissue curves from 3 × 3 pixel blocks.[15] Postprocessing of CTA-SI was performed by the CT technologists at the CT operator console. CTA source image reformats were 4-mm thick with a 2-mm gap. A follow-up MR imaging was performed on all patients 5–7 days following presentation, comprising, minimally, the following: DWI, 8125/minimum milliseconds (TR/TE), 26-cm FOV, 128 × 128 matrix, 5-mm section thickness, and no gap; and fluid-attenuated inversion recovery, 8000/120/200 ms (TR/TE/TI), 22-cm FOV, 320 × 224 matrix, 5-mm section thickness, and 1-mm gap.

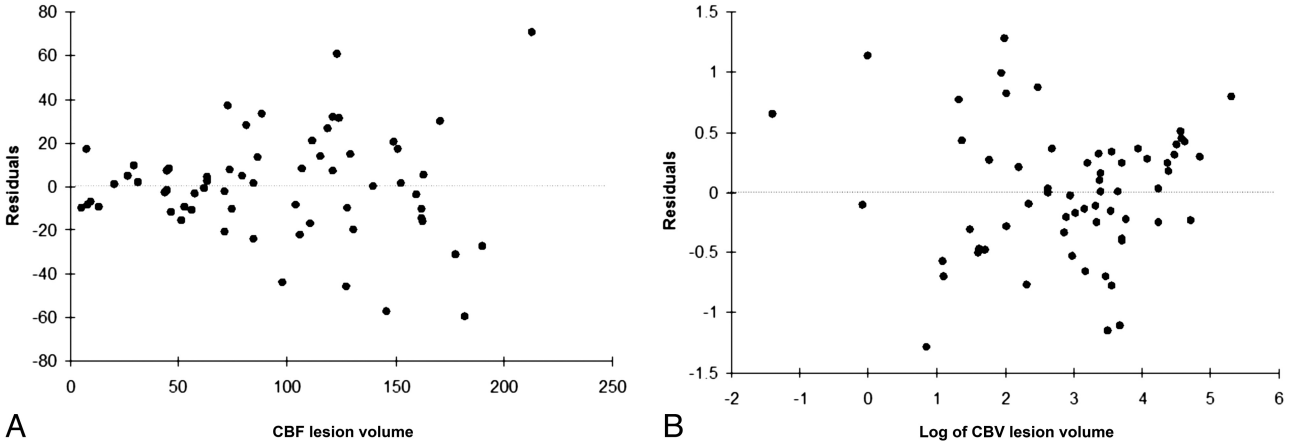

Fig 2. Plots of residuals for CBF defect volumes (*A*) and logCBV defect volumes (*B*) based on the linear regression equation. The residual is the difference between the predicted and actual observed value.

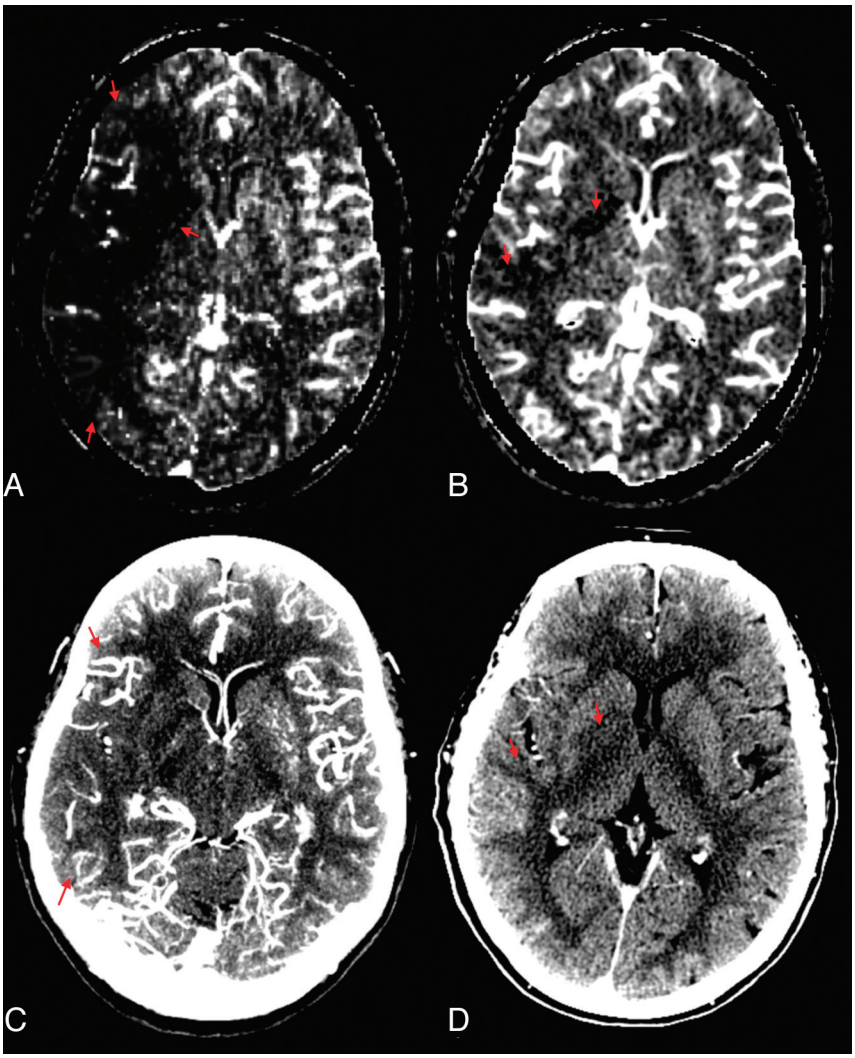

Fig 3. CBF (*A*) and CBV (*B*) maps. *C*, The hypoattenuation of CTA source image and gray-white matter differentiation loss correspond more closely with the CBF than with the CBV map. *D*, PCCT hypoattenuation corresponds most closely with CBV defect.

Image Postprocessing and Review Protocol

Before image review, anonymized images were transferred to a standalone server. PCCT and CTA-SI of each patient were coregistered with their own average perfusion CT images with SPM 5.0 (Wellcome Department of Imaging Neuroscience, London, United Kingdom) using the normalized mutual information function. Each registration was manually checked by an experienced research assistant (with 2 years' experience) by using the 3D voxel module in Analyze 8.0 (Biomedical Imaging Resonance; Mayo Clinic, Rochester, Minnesota). CTA-SI and perfusion CT were traced by an experienced neuroradiologist (R.I.A., with 6 years' experience) in a nonsequential manner blinded to perfusion CT data. Similarly perfusion CT, CBF, and CBV abnormalities were assessed by a second experienced neuroradiologist (S.S., with 7 years' experience). The final infarct measured at days 5–7 on follow-up MR imaging was traced by a third reader blinded to prior results (M.S., with 1 year's experience). Tracing was performed within Medical Image Processing, Analysis and Visualization, Version 4.0.2-2007-12-12 (Center for Information Technology, National Institutes of Health, Bethesda, Maryland). Subsequently, volumes for PCCT, CTA-SI, CBF, and CBV were added to the clinical data base (by M.S.), and analyses were performed.

Statistical Analysis

Results were expressed as mean (± SD) or median with interquartiles (Q1–Q3) for continuous variables, and frequency and proportion for categoric findings. Normal histogram methods were used to check normality for variables of CTA-SI, CBF, CBV, and PCCT. Natural log transformation was used for normalization of the distribution in which a normality check failed. Spearman correlation (r) was used to examine the association between lesion volumes of CTA-SI, CBF, CBV, and PCCT. Univariate linear regression analysis was used to look for the following relationships: between CTA-SI and CBF, between CTA-SI and CBV, between PCCT and CBF, or between PCCT and CBV. From the univariate linear regression model, predicted values and residuals were calculated individually. Residual plots were generated to evaluate linear regression models. The residual was defined as the difference between the predicted and the actual observed value based on the regression equation. Positive residual values occur when the observed value exceeds the predicted value. We considered observations as positive or negative outliers if the residual was greater than Q3 + 0.5 × IQR or less than Q1 − 0.5 × IQR, where Q1 and Q3 were the interquartiles of residuals and IQR was the interquartile range.

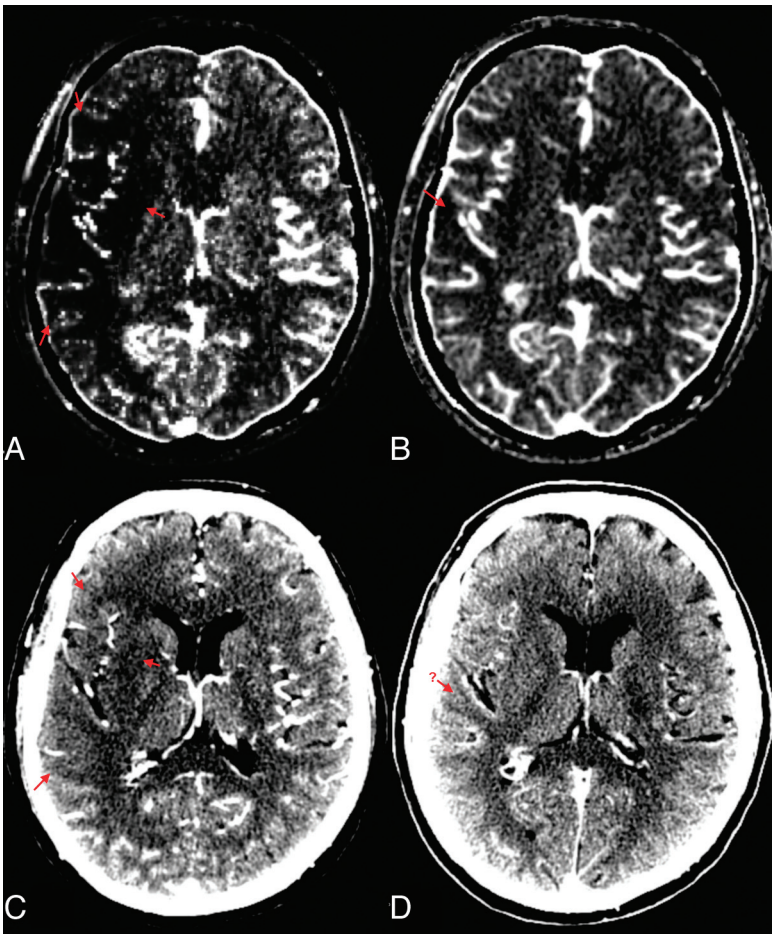

Fig 4. CBF map (*A*) reveals a large defect within the right MCA territory, while the CBV map (*B*) shows a substantially smaller region of infarction. *C*, CTA source image show hypoattenuation and gray-white matter differentiation loss in the right MCA territory corresponding to the CBF defect. *D*, PCCT image demonstrates subtle questionable posterior Sylvian hypoattenuation.

To search for significant baseline variables predictive of positive or negative outliers for CBF and CBV, we performed the Wilcoxon rank sum test (for continuous variables) and the Fisher exact test (for categoric variables), respectively. *P* values were adjusted for multiple comparisons of 8 baseline variables (age, sex, rtPA, ASPECTS, NIHSS score, onset to CT scan, time of bolus trigger to midinfarct, and recanalization) by using the Bonferroni adjustment. Positive and negative outliers were evaluated for differences in the site of vessel occlusion. ICA and M1 segment occlusions were considered proximal, whereas M2-M4 segment occlusions were considered distal. The Fisher exact test was used to compare differences in vessel occlusion between positive and negative outliers. All calculations were conducted within SAS software, Version 9.2 for Windows (SAS Institute, Cary, North Carolina).

Results

The mean ± SD were documented, and 47 patients, including all outliers, had proximal vessel occlusions. Segments involved were the following: 7 ICA segments (11%), 14 ACA (21.9%); MCA: M1 proximal, 26 (40.7%); M1 mid/distal, 39 (60.9%); M2, 55 (85.9%); M3, five (7.8%); and M4, three (4.7%). A mean rtPA dose of 61 ± 19 mg was administered in 46 patients. The median (IQR) CTA source image, PCCT, CBF, and CBV volumes of abnormality were 81.8 cm^3 (47.7–124.1 cm^3), 35.3 cm^3 (15.2–46.5 cm^3), 93.2 cm^3 (55.4–133.1 cm^3), and 37.5 cm^3 (7.6–41.0 cm^3), respectively. CTA-SI and CBF were normally distributed ($P = .15$ for CTA-SI or CBF), whereas PCCT and CBV were not normally distributed ($P = .01$ for PCCT or CBV), requiring normalization by natural log transformation. Spearman correlation demonstrated a strong positive correlation between CTA-SI with CBF ($r = 0.89$, $P < .0001$) and between PCCT and CBV ($r = 0.79$, $P < .0001$). Poorer CTA-SI to CBV ($r = 0.5$; $P < .0001$) and PCCT to CBF ($r = 0.52$, $P < .0001$) correlations were demonstrated.

From the linear regression model of CTA-SI on CBF and log-transformed PCCT on log-transformed CBV, the regression equations obtained were CTA-SI = 12.15 + 0.796 × CBF and log(PCCT) = 1.50 + 0.583 × log(CBV), respectively. The scatterplots with fitted linear regression lines are demonstrated in Fig 1*A*, -*B*. The residual is illustrated in Fig 2*A*, -*B*. The interquartiles (Q1, Q3) of residuals and the IQR from the regression model of CTA-SI and CBF were −10.76 and 11.42, and 22.18, respectively. Residuals >22.51 or <−21.85 were found in 17 (26.6%) patients who were considered positive or negative outliers. Similarly the Q1, Q3, and IQR of residuals from the PCCT and CBV regression models were −0.61, 0.61, and 1.21. Values >1.21 or <−1.21 were detected in 16 (25.0%) patients and designated as positive or negative outliers. Online Tables 1 and 2 compare baseline demographics between patients with positive outliers and patients with nonoutliers,

and between patients with negative outliers and patients with nonoutliers from the models of CTA-SI and CBF and PCCT and CBV, respectively. Positive outliers demonstrated a lower ASPECTS consistent with more severe infarcts. Positive outliers had a slightly larger baseline CBV (57.8 ± 14.9 versus 43.7 ± 14.8) and CBF volumes (139 ± 41.2 versus 123 ± 44.5) than negative outliers, though differences were not significant ($P = .47$ and $P = .59$ respectively). Both positive and negative outliers had higher NIHSS values than nonoutliers, though this did not reach clinical significance. Comparison of baseline volumes of CTA-SI demonstrated that positive outliers were more likely to have a larger baseline CTA source image (149 ± 46 cm^3 versus 83 ± 32 cm^3; $P = .002$, respectively) and final infarct (190 ± 100 cm^3 versus 80 ± 50 cm^3; $P = .09$, respectively) than nonoutliers. No baseline features were significantly related to PCCT outliers. There was no significant difference in the site of vessel occlusion for positive or negative outliers for CTA-SI or PCCT ($P = .55$ and $P = 1.00$, respectively).

Discussion

Our results demonstrate that hypoattenuation volumes of CTA-SI correlate highly with perfusion CT–measured CBF rather than CBV volumes (Figs 3 and 4). Positive outliers of CTA-SI presented with more severe infarcts and were manifest clinically and radiologically by lower ASPECTS and more extensive baseline CTA-SI and final infarct volumes than nonoutliers. Although not significantly different, positive outliers of CTA-SI presented earlier and had larger CBV and CBF abnormalities than negative outliers, suggesting more extensive baseline tissue at risk. The site of vessel occlusion was not significantly different between the groups. Early studies of CTA-SI, by using older CT scanners, assumed that a steady-state of arterial and tissue contrast was achieved during the scan acquisition.[16-18] Blood volume weighting was facilitated by lower contrast-injection rates, relatively long prep-delay times, and longer scanning times.[18] In a recent work, it has been suggested that the steady-state assumption no longer holds true with newer and faster MDCT CTA protocols. Injection rates of 5–7 mL/s and short prep-delay times of 15–20 seconds change the temporal shape of the time-attenuation curve, eliminating the near steady-state during acquisition of CTA-SI. Hence, with the current CTA implementation on faster state-of-the-art MDCT scanners, the CTA-SI are more flow- than volume-weighted.[19]

NCCT remains the technique of choice for imaging of acute stroke because it is fast and widely available and easily excludes other pathologies such as intracranial hemorrhage, even with less experienced readers. The sensitivity for detecting early ischemic signs is, however, limited and reported to be 40%–60%.[20-25] Infarct detection may be improved through the use of stroke windows[26] and standardized review such as ASPECTS.[3,4] The introduction of an operational definition of penumbra or potentially salvageable tissue and the wider availability of thrombolysis have laid the foundation for multimodal CT assessment of patients with stroke. Sensitivity for stroke detection by using such approaches is reported to be 78.9%, superior to NCCT (55.3%), CTA (57.9%), and perfusion CT (76.3%).[7] It is now generally agreed that admission CTA and perfusion CT significantly improve accuracy in infarct detection and delineation compared with NCCT alone.[26]

CTA-SI are thin-section reconstructions from CTA source data. They are important adjuncts to acute stroke imaging assessment, increasing CT accuracy for infarct detection, especially in the absence of DWI imaging.[5,10,11,26] CTA-SI have the advantage of whole-brain coverage as opposed to perfusion CT maps on the most prevalent scanners[12] and are available at scan completion with minimal usually automated console-generated postprocessing.[27] CTA-SI are reported as more sensitive for the detection of early irreversible ischemia, with a sensitivity of 70% compared with 48% for NCCT.[6]

Hypoattenuation on CT and CTA-SI is pathophysiologically distinct. Hypoattenuation seen on NCCT correlates with severe hypoperfusion and decreased proton diffusion representing irreversible ischemic injury.[23,28] NCCT hypoattenuation is due to extra- to intracellular shift of brain tissue water, whereas hypoattenuation of CTA-SI most likely reflects reduction in blood and, therefore, contrast distribution to the affected territory.[9]

Several earlier studies have suggested that CTA-SI are volume-weighted. Coutts et al[9] reported greater sensitivity of CTA-SI to ischemic changes, more accurately predicting the volume of final infarct. A further study of 28 patients confirmed that NCCT, CTA-SI, and CBV maps represent unsalvageable tissue despite reperfusion.[12] Lev et al[11] correlated the volume of abnormality of CTA-SI most closely with that of final infarct volume in the presence of prompt recanalization. Camargo et al[6] reported CTA-SI to be more accurate in predicting final infarct volume ($R^2 = 0.73$). Finally the American Heart Association Guidelines report that CTA-SI provide a qualitative CBV map reflecting infarct core.[27] Our findings are important clinically because if CTA-SI acquired on modern scanners are used to identify infarct core, as suggested by multiple prior studies and American Heart Association Guidelines, then tissue at risk is likely to be overestimated. This could erroneously lead to fewer patients being eligible for thrombolysis. Additionally, the expanded coverage provided by CTA-SI now provides the treating physician with a whole-head estimate of tissue at risk. This may reduce the number of ischemic lesions missed due to inadequate coverage.[29,30]

A potential limitation of our study was the use of individual readers, each delineating either CTA-SI/PCCT or CBF/CBV extent. The purpose of the study was not to test interobserver agreement of our observations but to assess the flow- or volume-weighting of hypoattenuation of CTA-SI. The use of 2 different expert readers for the CTA-SI/PCCT and perfusion tracings, combined with the blinded and nonsequential review by each reader, together with the relatively large sample size, precluded any observational or recall bias. We did not correlate CTA-SI findings with final infarct on delayed imaging. We reasoned that the final infarct is dependent on a number of confounding factors, including but not limited to recanalization, time to presentation and treatment, thrombolysis administration, collateral circulation, and blood pressure. Both CTA-SI and perfusion imaging are obtained minutes apart at baseline. We believe that direct comparison more accurately reflects the relationship between the 2 sequences and provides a quantitative assessment independent of clinical confounders.

Conclusions

The results of our study support the hypothesis that currently implemented CTA source image protocols are CBF- rather than CBV-weighted.

References

1. Parsons MW, Pepper EM, Chan V, et al. **Perfusion computed tomography: prediction of final infarct extent and stroke outcome.** *Ann Neurol* 2005; 58:672–79
2. Wardlaw JM, Farrall AJ. **Diagnosis of stroke on neuroimaging.** *BMJ* 2004;328:655–56
3. Demchuk AM, Hill MD, Barber PA, et al. **Importance of early ischemic computed tomography changes using ASPECTS in NINDS rtPA Stroke Study.** *Stroke* 2005;36:2110–15. Epub 2005 Sep 15
4. Dzialowski I, Hill MD, Coutts SB, et al. **Extent of early ischemic changes on computed tomography (CT) before thrombolysis: prognostic value of the Alberta Stroke Program Early CT Score in ECASS II.** *Stroke* 2006;37:973–78
5. Schramm P, Schellinger PD, Fiebach JB, et al. **Comparison of CT and CT angiography source images with diffusion-weighted imaging in patients with acute stroke within 6 hours after onset.** *Stroke* 2002;33:2426–32
6. Camargo EC, Furie KL, Singhal AB, et al. **Acute brain infarct: detection and delineation with CT angiographic source images versus nonenhanced CT scans.** *Radiology* 2007;244:541–48
7. Kloska SP, Nabavi DG, Gaus C, et al. **Acute stroke assessment with CT: do we need multimodal evaluation?** *Radiology* 2004;233:79–86
8. Warach S, Wardlaw J. **Advances in imaging 2005.** *Stroke* 2006;37:297–98
9. Coutts SB, Lev MH, Eliasziw M, et al. **ASPECTS on CTA source images versus unenhanced CT: added value in predicting final infarct extent and clinical outcome.** *Stroke* 2004;35:2472–76
10. Aviv RI, Shelef I, Malam S, et al. **Early stroke detection and extent: impact of experience and the role of computed tomography angiography source images.** *Clin Radiol* 2007;62:447–52
11. Lev MH, Segal AZ, Farkas J, et al. **Utility of perfusion-weighted CT imaging in acute middle cerebral artery stroke treated with intra-arterial thrombolysis: prediction of final infarct volume and clinical outcome.** *Stroke* 2001;32: 2021–28
12. Lin K, Rapalino O, Law M, et al. **Accuracy of the Alberta Stroke Program Early CT Score during the first 3 hours of middle cerebral artery stroke: comparison of noncontrast CT, CT angiography source images, and CT perfusion.** *AJNR Am J Neuroradiol* 2008;29:931–36
13. Konstas AA, Goldmakher GV, Lee TY, et al. **Theoretic basis and technical implementations of CT perfusion in acute ischemic stroke. Part 2. Technical implementations.** *AJNR Am J Neuroradiol* 2009;30:885–92
14. Lee TY, Stewart E. **Scientific basis and validation.** In: Miles KA, Charnsangavej C, Cuenod CA, eds. *Multidetector Computed Tomography in Oncology: CT Perfusion Imaging.* London, UK: Informa Healthcare; 2007:15–46
15. Johnson JA, Wilson TA. **A model for capillary exchange.** *Am J Physiol* 1966;210:1299–303
16. Axel L. **Cerebral blood flow determination by rapid-sequence computed tomography: theoretical analysis.** *Radiology* 1980;137:679–86
17. Hamberg LM, Hunter GJ, Kierstead D, et al. **Measurement of cerebral blood volume with subtraction three-dimensional functional CT.** *AJNR Am J Neuroradiol* 1996;17:1861–69
18. Hunter GJ, Hamberg LM, Ponzo JA, et al. **Assessment of cerebral perfusion and arterial anatomy in hyperacute stroke with three-dimensional functional CT: early clinical results.** *AJNR Am J Neuroradiol* 1998;19:29–37
19. Konstas AA, Goldmakher GV, Lee TY, et al. **Theoretic basis and technical implementations of CT perfusion in acute ischemic stroke. Part 1. Theoretic basis.** *AJNR Am J Neuroradiol* 2009;30:662–68
20. Tomura N, Uemura K, Inugami A, et al. **Early CT finding in cerebral infarction: obscuration of the lentiform nucleus.** *Radiology* 1988;168:463–67
21. Truwit CL, Barkovich AJ, Gean-Marton A, et al. **Loss of the insular ribbon: another early CT sign of acute middle cerebral artery infarction.** *Radiology* 1990;176:801–06
22. von KR, Meyding-Lamade U, Forsting M, et al. **Sensitivity and prognostic value of early CT in occlusion of the middle cerebral artery trunk.** *AJNR Am J Neuroradiol* 1994;15:9–15
23. von Kummer R, Bourquain H, Bastianello S, et al. **Early prediction of irreversible brain damage after ischemic stroke at CT1.** *Radiology* 2001;219:95–100
24. Patel SC, Levine SR, Tilley BC, et al. **Lack of clinical significance of early ischemic changes on computed tomography in acute stroke.** *JAMA* 2001;286: 2830–38
25. Lev MH, Farkas J, Gemmete JJ, et al. **Acute stroke: improved nonenhanced CT detection–benefits of soft-copy interpretation by using variable window width and center level settings.** *Radiology* 1999;213:150–55
26. Ezzeddine MA, Lev MH, McDonald CT, et al. **CT angiography with whole brain perfused blood volume imaging: added clinical value in the assessment of acute stroke.** *Stroke* 2002;33:959–66
27. Latchaw RE, Alberts MJ, Lev MH, et al. **Recommendations for imaging of acute ischemic stroke: a scientific statement from the American Heart Association.** *Stroke* 2009;40:3646–78
28. Sobesky J, von Kummar R, Frackowiak M, et al. **Early ischemic edema on cerebral computed tomography: its relation to diffusion changes and hypoperfusion within 6 h after human ischemic stroke—a comparison of CT, MRI and PET.** *Cerebrovasc Dis* 2006;21:336–39
29. Wintermark M, Fischbein NJ, Smith WS, et al. **Accuracy of dynamic perfusion CT with deconvolution in detecting acute hemispheric stroke.** *AJNR Am J Neuroradiol* 2005;26:104–12
30. Rai AT, Carpenter JS, Peykanu JA, et al. **The role of CT perfusion imaging in acute stroke diagnosis: a large single-center experience.** *J Emerg Med* 2008;35: 287–92